Supporting information

Dynamics of a Key Conformational Transition in the Mechanism of Peroxiredoxin Sulfinylation

by

Alexandre Kriznik[1,2], Marouane Libiad[3], Hélène Le Cordier[1], Samia Boukhenouna[1], Michel B Toledano[3] & Sophie Rahuel-Clermont[1,2]*

[1] IMoPA, Université de Lorraine, CNRS, Biopole, Campus Biologie Santé, F-54000 Nancy, France

[2] UMS2008 IBSLor, Biophysics and Structural Biology core facility, Université de Lorraine, CNRS, INSERM, Biopole, Campus Biologie Santé, F-54000 Nancy, France

[3] Institute for Integrative Biology of the Cell (I2BC), UMR9198, CNRS, CEA-Saclay, Université Paris-Saclay, iBiTecS/SBIGEM, Laboratoire Stress oxydant et Cancer, Bat 142, F-91198 Gif-sur-Yvette Cedex, France

* E-mail: sophie.rahuel@univ-lorraine.fr

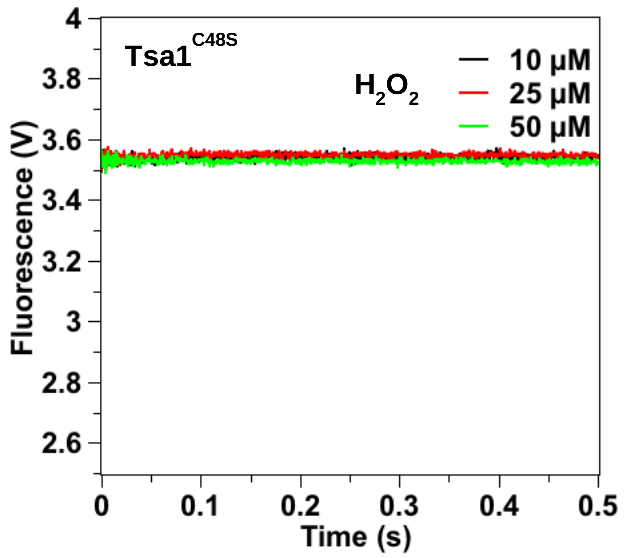

Figure S1. Pre-steady state kinetics for the reaction of Tsa1^{C48S} (5 µM) with increasing H_2O_2 (10, 25, 50 µM) monitored by Trp fluorescence as in Fig. 2b.

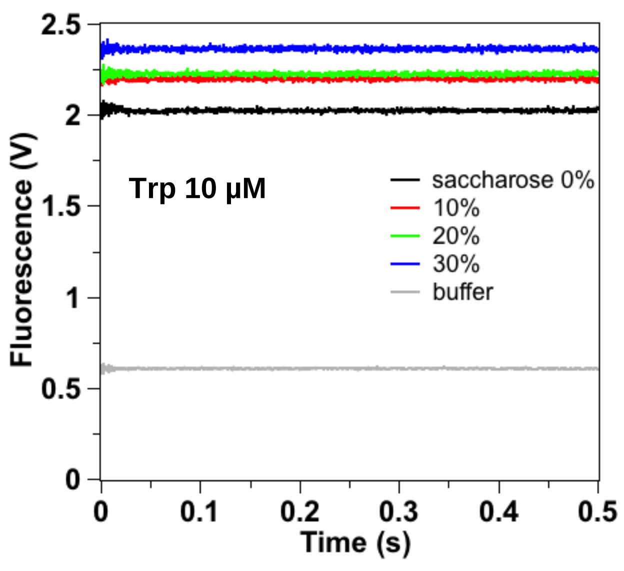

Figure S2. Test of stop flow mixer efficiency in viscous solutions, based on the effect of saccharose (0% black, 10 % red, 20% green and 30% blue) on Trp amino-acid fluorescence (10 µM) monitored as in Fig. 2b.

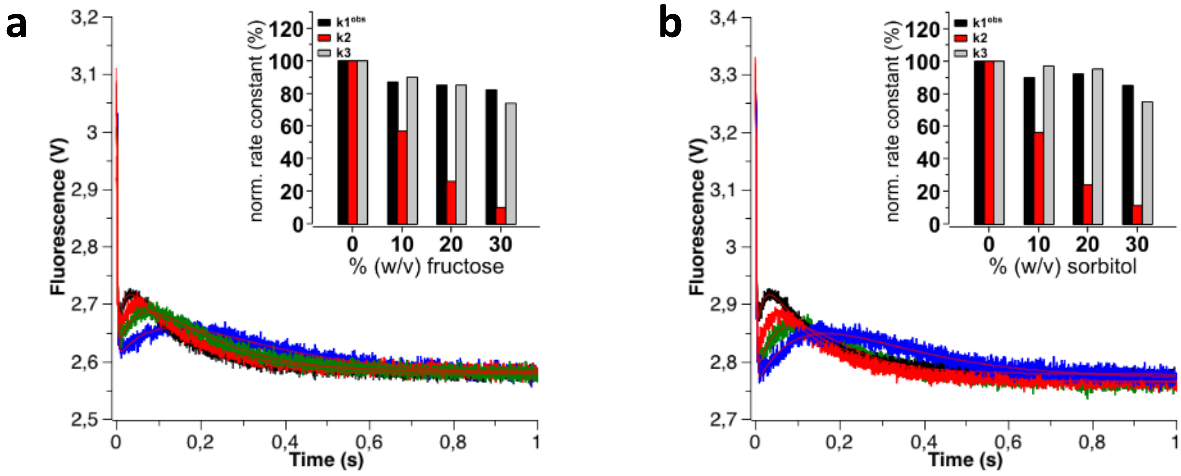

Figure S3. Effect of viscogens fructose (a) and sorbitol (b) (0% black, 10 % red, 20% green and 30% blue) on the reaction of Tsa1 (5 µM) with H_2O_2 (10 µM) monitored as in Fig. 2, fitted against a 3-exponential equation (red lines). Insets, effect of viscogen concentration on rate constants $k1^{obs}$, k2 and k3 normalized to 0% viscogen.

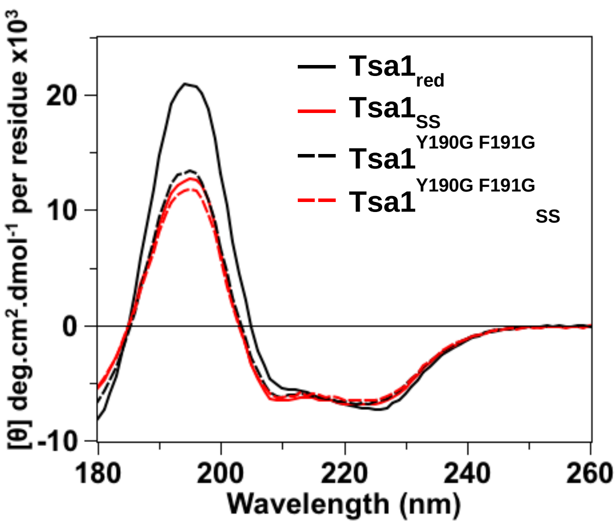

Figure S4. Far-UV CD spectra of 5 µM wild-type Tsa1 (plain) and $Tsa1^{Y190G\ F191G}$ (dash line) under the reduced (black) and disulfide (red) forms. Measurements were performed in a 0.01 cm flat cell in phosphate (10 mM) NaF (100 mM) buffer pH 7 and are the average of three records.

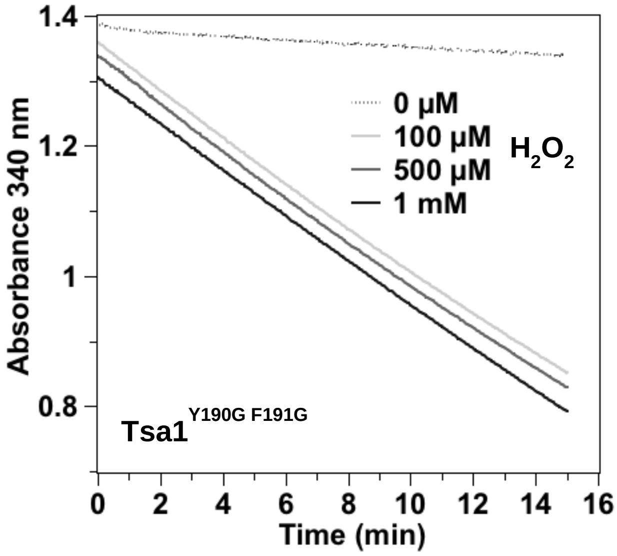

Figure S5. Steady state kinetics for the determination of the hyperoxidation sensitivity of Tsa1$^{Y190G\ F191G}$ with H_2O_2 monitored by consumption of NADPH (200 µM) at 340 nm in the presence *E. coli* thioredoxin reductase (0.25 µM), *E. coli* Trx1 (5 µM), Tsa1 (1 µM) and variable amounts of H_2O_2 (from 100 µM to 1 mM) in TK buffer. The time courses have been shifted on the y-axis for clarity.

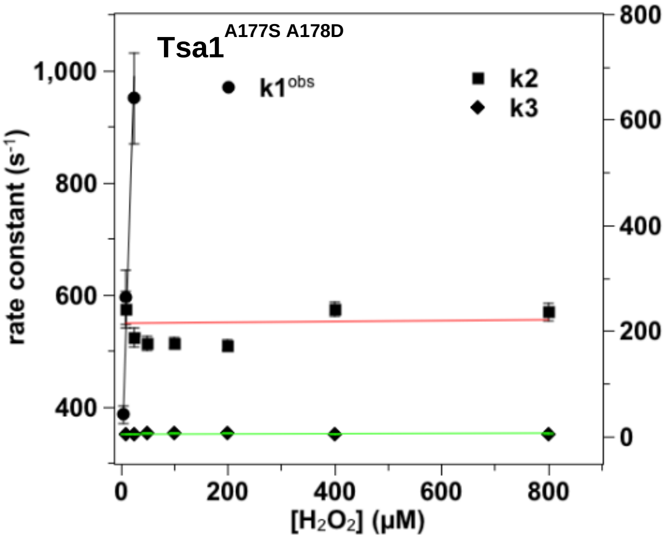

Figure S6. Second order plots and linear fits of the observed rate constants $k1^{obs}$ (circles, black line), k2 (squares, red line) and k3 (diamond, green line) for Tsa1$^{A177S\ A178D}$ reaction kinetics with H_2O_2.

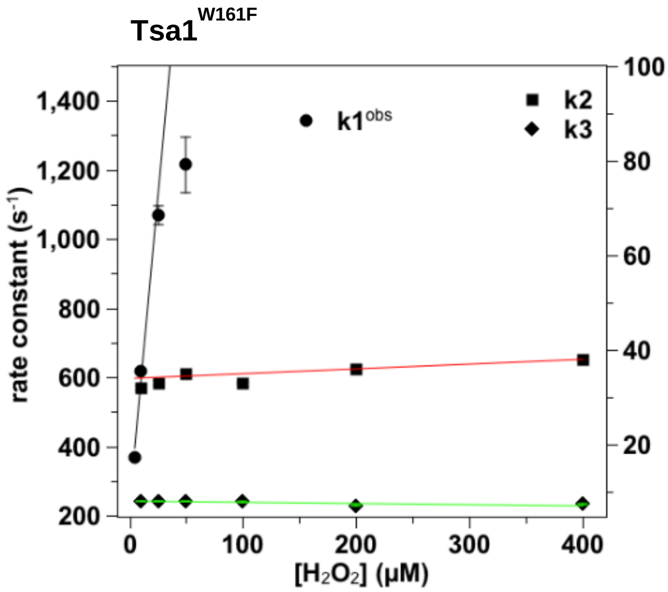

Figure S7. Second order plots and linear fits of the observed rate constants $k1^{obs}$ (circles, black line), k2 (squares, red line) and k3 (diamond, green line) for $Tsa1^{W161F}$ reaction kinetics with H_2O_2.

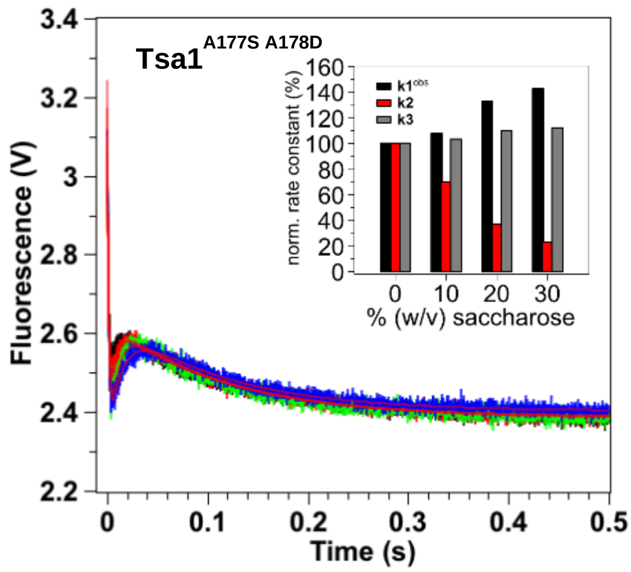

Figure S8. Effect of saccharose (0% black, 10 % red, 20% green and 30% blue) on the reaction of $Tsa1^{A177S\ A178D}$ (5 μM) with H_2O_2 (10 μM) monitored as in Fig. 2b, fitted against a 3-exponential equation (red line). Inset, effect of saccharose concentration on rate constants $k1^{obs}$, k2 and k3 normalized to 0% saccharose.

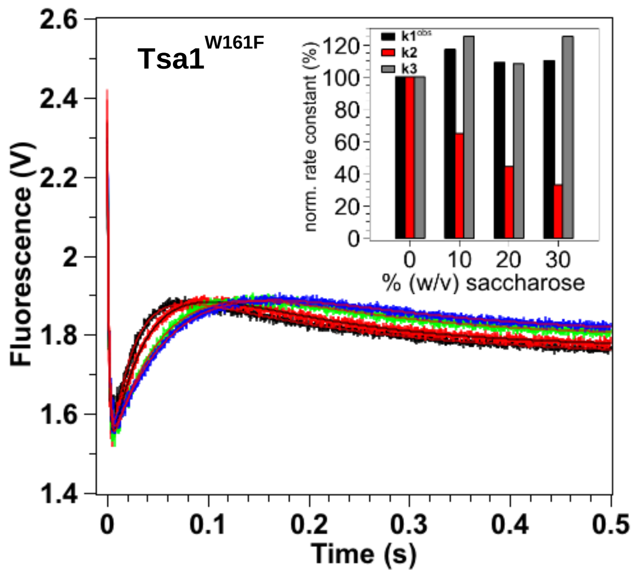

Figure S9. Effect of saccharose (0% black, 10 % red, 20% green and 30% blue) on the reaction of Tsa1^{W161F} (5 µM) with H_2O_2 (10 µM) monitored as in Fig. 2b, fitted against a 3-exponential equation (red or black line). Inset, effect of saccharose concentration on rate constants k1^{obs}, k2 and k3 normalized to 0% saccharose.

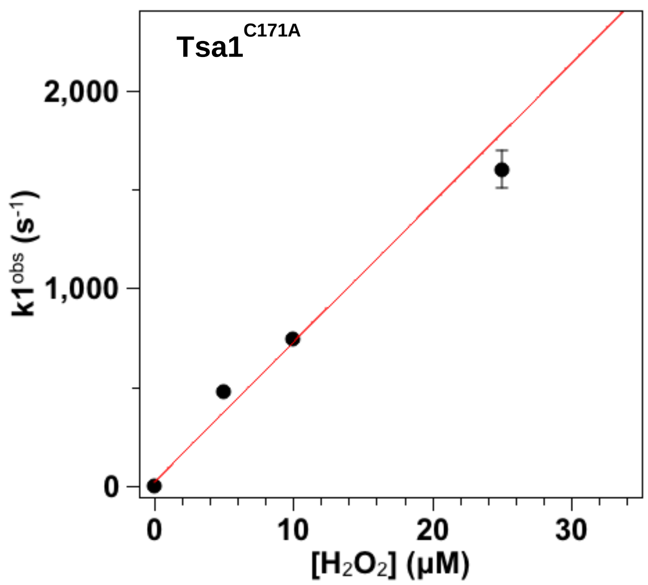

Figure S10. Second order plot and linear fit of the observed rate constants k1^{obs} *vs* H_2O_2 concentration, for the reaction kinetics of Tsa1^{C171A} with H_2O_2.

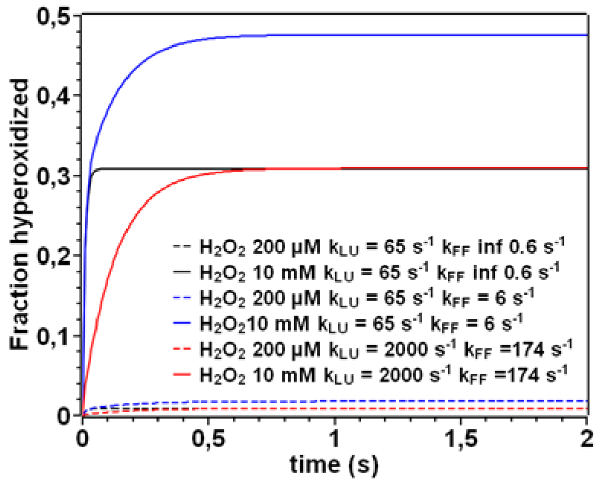

Figure S11. Simulation of the kinetics of formation of Tsa1$_{SO2}$. Simulations were performed based on the model from Figure 6b, using the fitted rate constants values k_{SOH} and k_{SO2} reported in Table 1 and the indicated values for k_{LU}, k_{FF} and H_2O_2 concentrations. Using fluorescence intensity factors of 62 and 124 % for Tsa1$_{SS}$ and Tsa1$_{SO2}$ respectively (Figure 2a), the fraction of Tsa1 in each state at completion of the reaction was estimated from Figure 6a data. At H_2O_2 concentrations of 200 µM and 10 mM, Tsa1$_{SO2}$ contributes to 1% and 30 % of the total, and Tsa1$_{SS}$ the remainder up to 100 % (black lines). Fixing k_{LU} at the fitted value of 65 s^{-1} and setting k_{FF} to values higher than 0.6 s^{-1} increased the hyperoxidized fraction to values incompatible with experimental observations. For instance, with k_{FF} = 6 s^{-1} Tsa1$_{SO2}$ reaches 2 and 48 % at 200 µM and 10 mM H_2O_2, respectively (blue lines). This supports that $k_{FF} << k_{LU}$.

To simulate the Tsa1^{FF}—SOH ⇆ Tsa1^{LU}—SOH in rapid equilibrium, k_{LU} was set at 2000 s^{-1}, in which case fractions of Tsa1$_{SO2}$ consistent with observation were obtained for k_{FF} = 174 $^{s-1}$ (red lines). However in this case the FF to LU conformational event would be too fast to be observed in fluorescence, and the rate constant of Tsa1$_{SO2}$ formation would be of ~5 s^{-1}, i.e. , mostly controlled by k_{SS}.

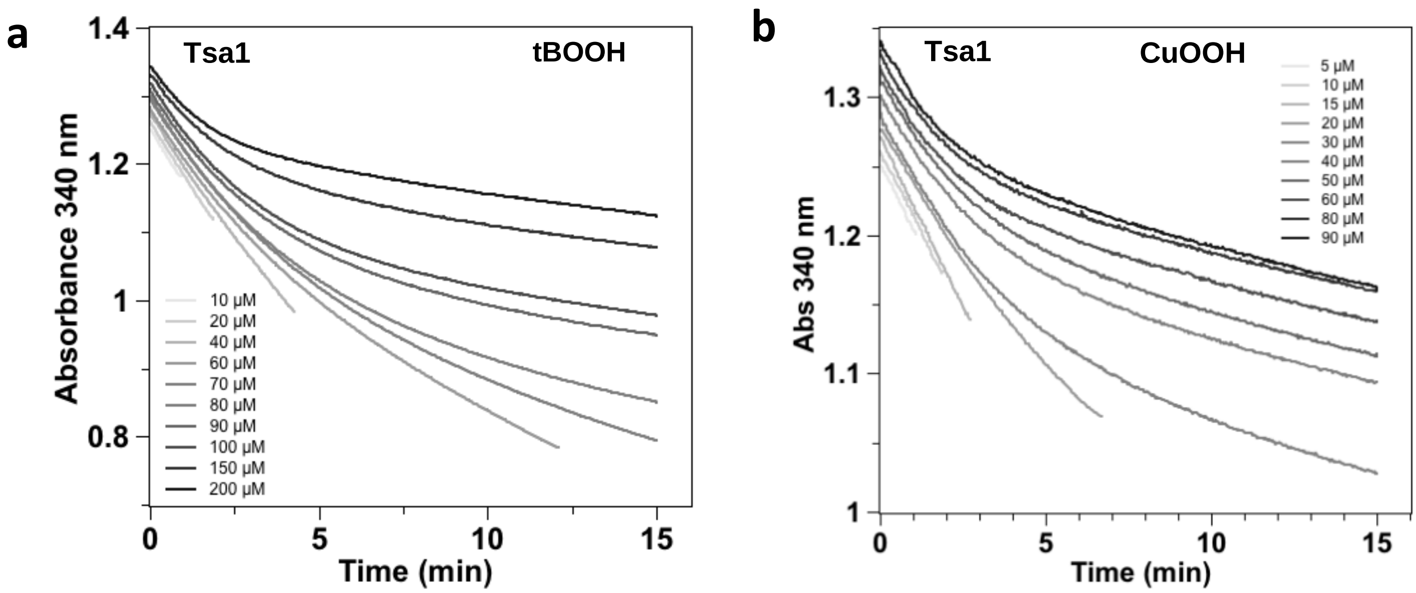

Figure S12. Steady state kinetics for the determination of hyperoxidation sensitivity of Tsa1 with tBOOH monitored by consumption of NADPH (200 µM) at 340 nm in the presence thioredoxin reductase (0.25 µM), Trx1 (5 µM), Tsa1 (1 µM) and variable amounts of (a) tBOOH (from 10 to 200 µM as indicated), and (b) CuOOH (as indicated). The time courses have been shifted on the y-axis for clarity.

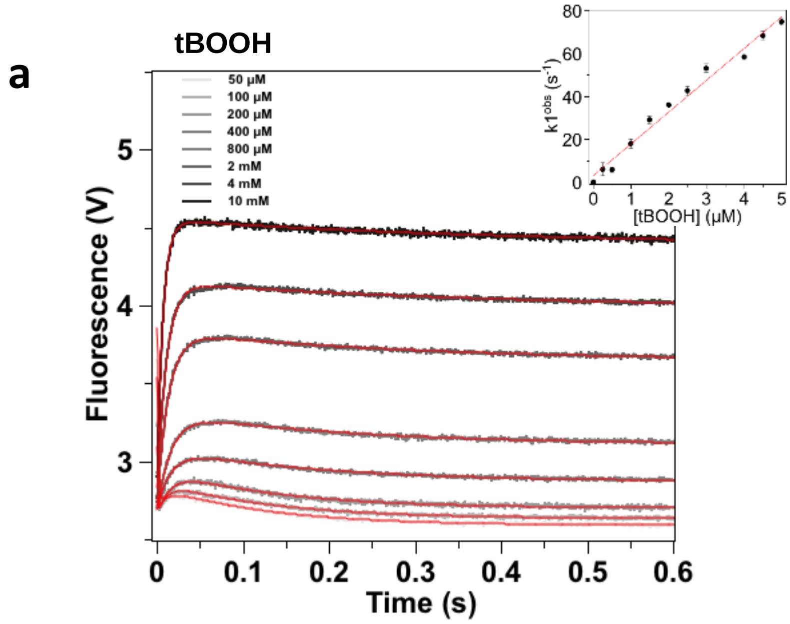

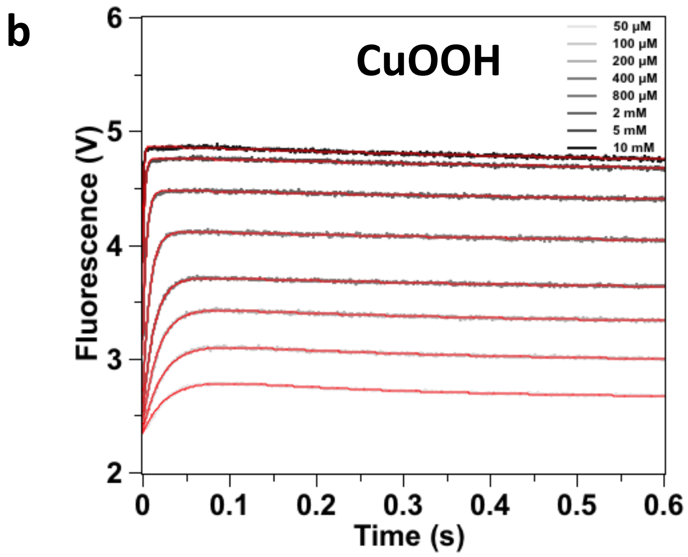

Figure S13. a. Pre-steady state kinetics for the reaction of Tsa1 (5 µM) with tBOOH (as indicated) monitored as in Fig. 2B, fitted against a multiexponential equation (red line). Inset, precise determination of k1 by second order plot and linear fit of the rate constants $k1^{obs}$ obtained from kinetics measured for the reaction of Tsa1 (0.5 µM) with low tBOOH concentrations (from 0.5 to 5 µM). b. Pre-steady state kinetics for the reaction of Tsa1 (5 µM) with CuOOH (as indicated) monitored as in Fig. 2B, fitted against a multiexponential equation (red line).

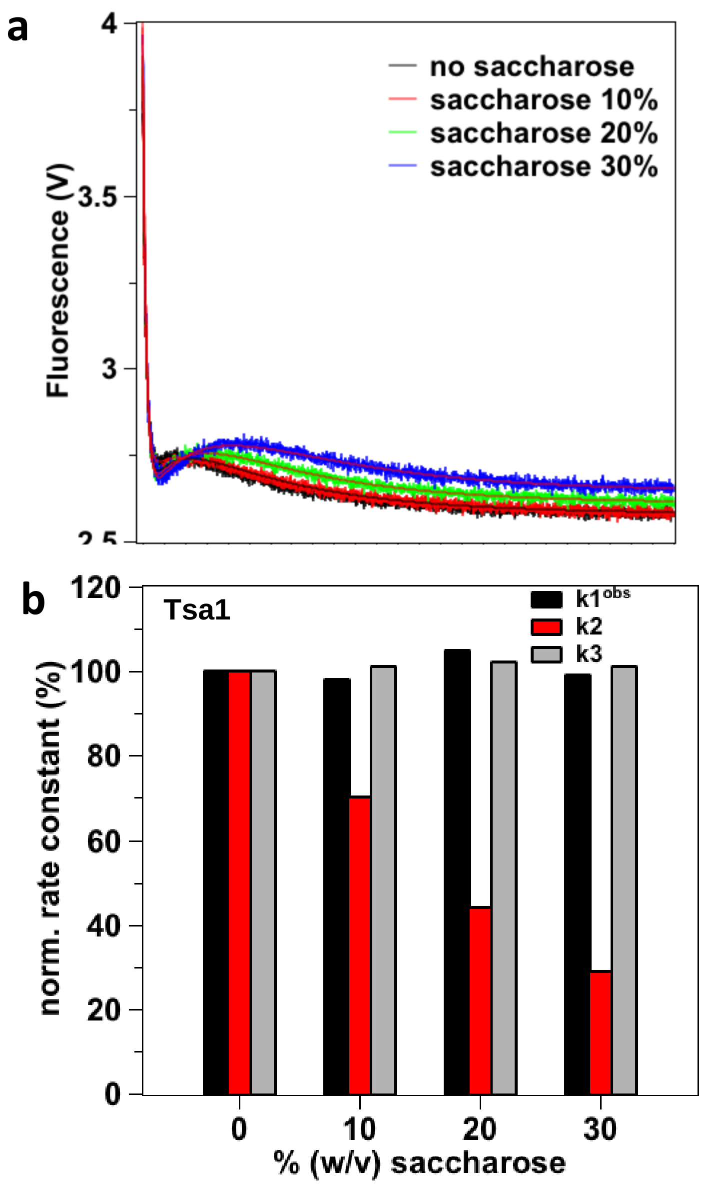

Figure S14. a, effect of saccharose (0% black, 10 % red, 20% green and 30% blue) on the reaction of Tsa1 (5 µM) with tBOOH (10 µM) monitored as in Fig. 2b, fitted against a 3-exponential equation (red or black line). b, effect of saccharose concentration on rate constants $k1^{obs}$, k2 and k3 normalized to 0% saccharose.

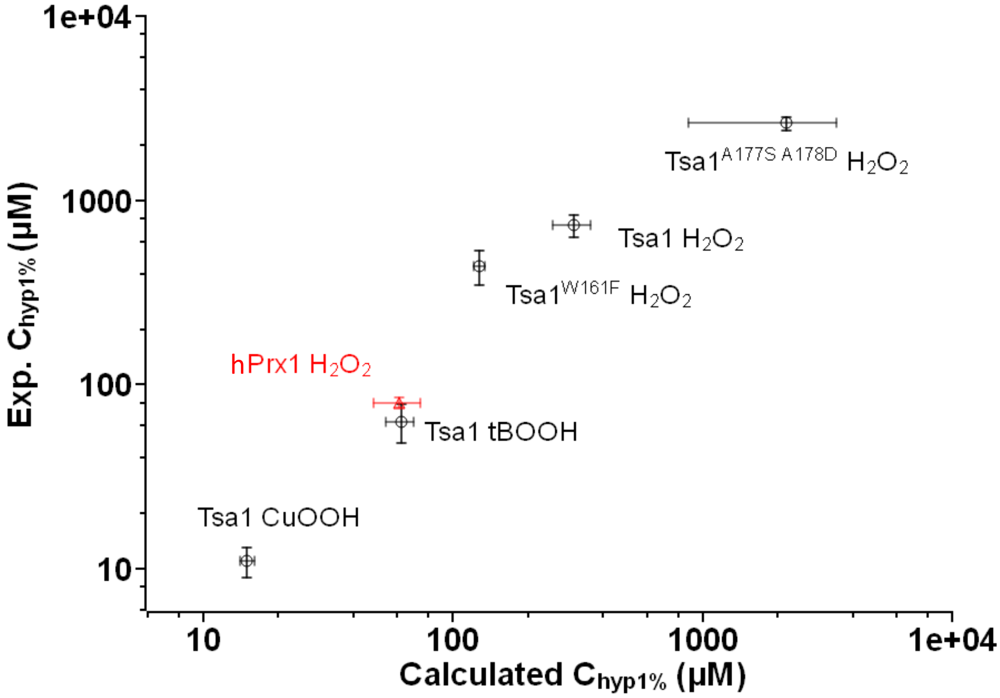

Figure S15. Comparison of the calculated and experimental $C_{hyp1\%}$ for wild-type and mutant Prxs

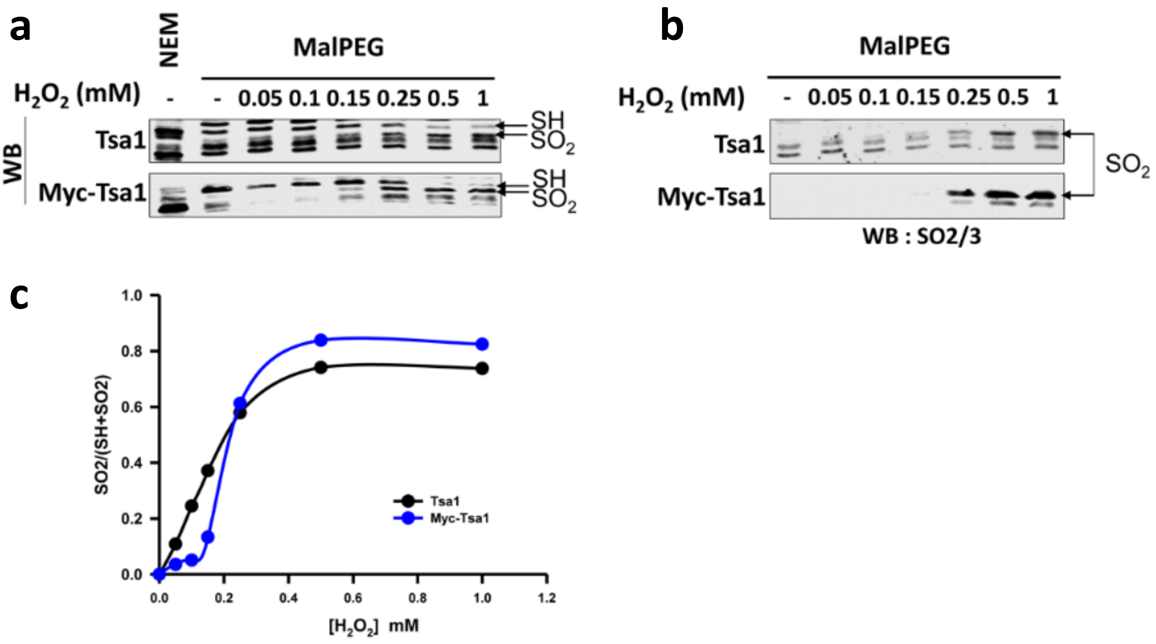

Figure S16. Validation of the mPEG differential cysteine derivatization procedure to monitor Prx hyperoxidation using N-terminal tagged Tsa1 (Myc-Tsa1), and comparison of the reactivity of Myc-Tsa1 and Tsa1 towards H_2O_2. a,b, Thiols were derivatized by NEM or mPEG, as indicated, after reduction with DTT, as described in methods, using cell lysates of Δ*tsa1* expressing human Tsa1 or Myc-Tsa1 and exposed to H_2O_2 at the indicated concentration. a, Western blot of reduced (-SH) (2 X mPEG) and hyperoxidized (-SO_2H) (1 X mPEG) forms of Tsa1 and Myc-Tsa1 (indicated by black arrows), revealed with an anti-Prx (Tsa1) or anti-Myc (Myc-Tsa1) antibody. Quantification of the degree of oxidation (SO_2H/ SH + SO_2H) is shown below the western blot (c). b, Western blot of the SO_2H forms of Tsa1 and Myc-Tsa1, using a Prx anti-$SO_{2/3}$ antibody and the cell lysates used in a.